Angew. Chem. Int. Ed. **2001**, *40* (6), 1102-1104

Three-Dimensional Transmission Electron Microscopy Observations of Mesopores in Dealuminated Zeolite Y**

Andries H. Janssen, Abraham J. Koster, Krijn P. de Jong*

[*] Prof. Dr. Ir. K.P. de Jong, Drs. A.H. Janssen
Department of Inorganic Chemistry and Catalysis
Debye Institute, Utrecht University
PO BOX 80083, 3508 TB Utrecht, The Netherlands
Fax: (+31) 30 251 1027
E-mail: k.p.dejong@chem.uu.nl
WWW: http://www.anorg.chem.uu.nl

Dr. A.J. Koster
Department of Molecular Cell Biology
Utrecht University
Padualaan 8, 3584 CH Utrecht, The Netherlands

[**] Supported by NWO under grant 98037. The research of AJK has been made possible by a fellowship of the Royal Netherlands Academy of Arts and Sciences (KNAW). The authors thank J.E.M.J. Raaymakers for the nitrogen physisorption measurements, A.J.M. Mens for the XPS measurements, J.A.R. van Veen and E.J. Creyghton for physical data and useful discussions and Shell International Chemicals and Zeolyst for the samples.

Zeolites are microporous crystalline aluminosilicates, which makes them very suitable for separation processes or shape selective catalysis. The micropores of zeolites are often advantageous to induce shape selectivity, but enhanced accessibility is frequently desirable to restrict mass transfer effects and/or allow catalytic conversion of larger molecules. Several approaches have been followed to enhance accessibility;[1] i.e. the development of zeolites with intrinsically larger pores,[2] delaminated zeolite precursors[3] and zeolite nanocrystals.[4] A widely applied method to enhance accessibility is the creation of materials with both micropores (<2 nm in diameter) and mesopores (2-50 nm in diameter). This can be done by special synthesis techniques[5] or by post-synthesis modification of zeolites with hydrothermal treatments (steaming) or acid leaching.[6] Steaming and acid leaching treatments generate mesopores by extraction of aluminum from the zeolite lattice, thus causing partial collapse of the framework. Up to now the characterization of these mesopores has been done with nitrogen physisorption and Transmission Electron Microscopy (TEM).[7] However, the visualization of the mesopores with conventional TEM gives no information about the shape, connectivity and three-dimensional orientation of the pores. Furthermore, often the zeolite crystals are cut in thin slices with an ultramicrotome to investigate the pores. This may cause fracturing of the zeolite crystal, which hinders the interpretation of the TEM images. Recently the mesoporous structure of MCM-48 has been determined by electron crystallography.[8] However, this method is suitable only for materials with well-ordered pores. With three-dimensional transmission electron

microscopy (3D-TEM) it is possible to image (random) mesopores of an intact zeolite crystal in three dimensions.[9] Here we show 3D-TEM results of the size, shape and connectivity of the mesopores in a series of (steamed/acid leached) Y zeolites. Moreover, a quantitative comparison between the 3D-TEM images and nitrogen physisorption is made. This enables us to propose a detailed model for the generation of mesopores.

3D-TEM, sometimes referred to as electron tomography,[10] is a technique where a series of 2D TEM images (scattering contrast) is recorded that is subsequently used to compute a 3D image (3D reconstruction) of the object under investigation.[9-12] By virtual cross sectioning of such a 3D reconstruction one can reveal the interior of the object. To study the generation of mesopores, we used a series of Y zeolites with increasing mesopore volume, *viz.* NaY, USY (Ultra Stable Y) and XVUSY (eXtra Very Ultra Stable Y). The USY sample is a steamed NH_4Y, whereas the XVUSY is steamed twice and severely acid leached. The physical properties of these samples are given in Table 1.

Table 1: Physical properties of NaY (CBV100), USY (CBV400) and XVUSY (CBV780)

	Si/Al bulk (at/at)	Si/Al XPS (at/at)	a_0 (nm)	%Y[a]	V_{micro}[b] (ml/g)	V_{micro} calc.[c] (ml/g)	V_{meso}[d] (ml/g)	S_T[e] (m^2/g)
NaY	2.6	2.8	2.469	100	0.341	0.341	0.053	8
USY	2.6	1.1	2.450	87	0.256	0.324	0.108	63
XVUSY	39.3	71.3	2.423	72	0.277	0.267	0.251	120

[a]Relative crystallinity [b]Micropore volume from t-plot; $t=[14.3600/(0.1013-\log(P/P_0))]^{0.5}$ [c]Expected micropore volume if all micropores are empty; calculated by correcting V_{micro} of NaY for crystallinity, a_0 and sodium weight of USY and XVUSY [d]V_{total}-V_{micro} [e] Sum of external and mesopore surface area calculated from t-plot[13]

In Figures 1-3 2D-TEM images and thin slices through the 3D-TEM reconstructions are shown for NaY, USY and XVUSY, respectively.

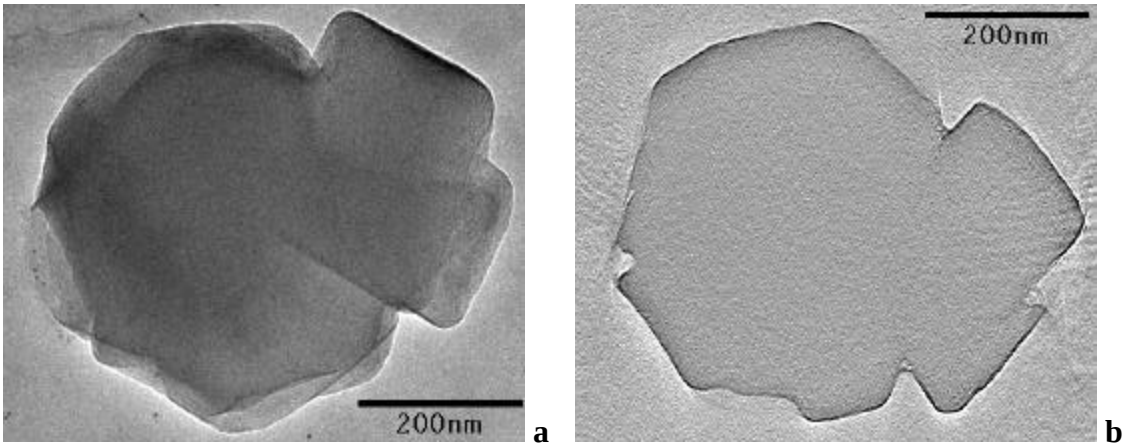

a **b**

Figure 1: 2D-TEM image of a NaY crystal taken at a magnification of 15kx (a) and a thin (1.7 nm) slice through the 3D-TEM reconstruction of this crystal (b).

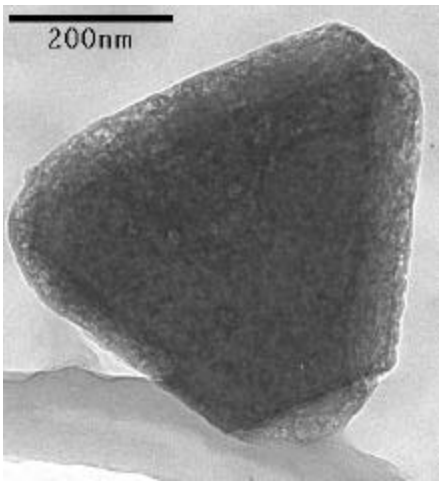

a

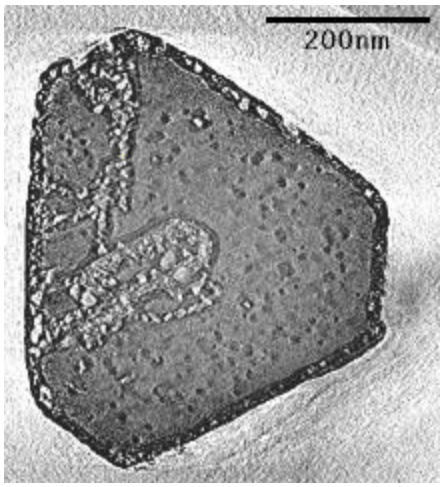

b

Figure 2: 2D-TEM image of a USY crystal taken at a magnification of 15kx (a) and a thin (1.7 nm) slice through the 3D-TEM reconstruction of this crystal (b).

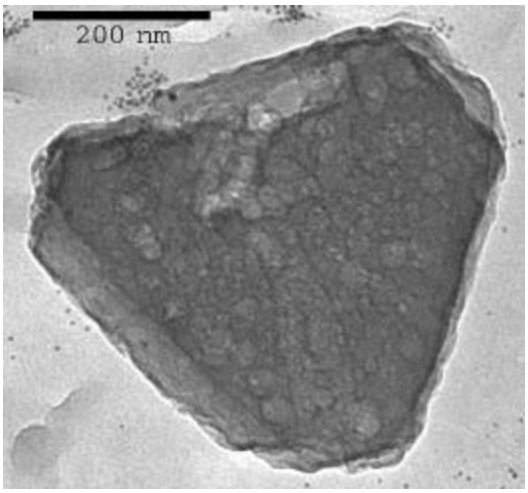

a

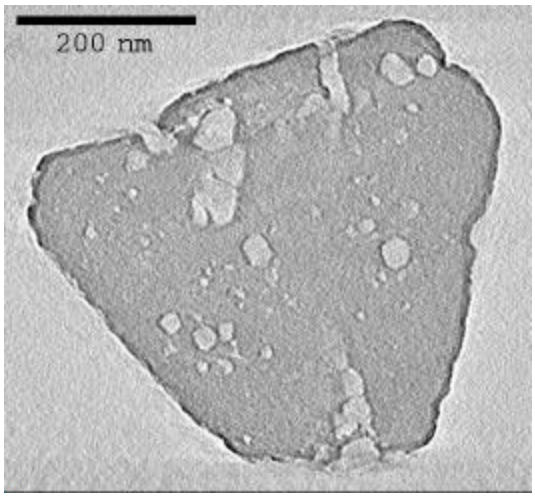

b

Figure 3: 2D-TEM image of an XVUSY crystal taken at a magnification of 20kx (a) and a thin (1.25 nm) slice through the 3D-TEM reconstruction of this crystal (b). Small gold particles (5 nm), used as markers, are observed in Figure 3a.

In the conventional TEM images the mesopores of USY and XVUSY are just visible as lighter areas, whereas in the thin slices through the 3D-TEM reconstructions of USY and XVUSY the mesopores can be distinguished very well as light areas. In line with the results from physisorption (Table 1) NaY does not show any mesopores in both the 2D- and 3D-TEM images; the same holds for NH_4Y (not shown). This indicates that the light areas in Figure 2b and 3b really are the mesopores and not an artifact of the reconstruction. The diameters of the mesopores visualized with 3D-TEM are 3-20 nm for USY and 4-34 nm for XVUSY. This is in excellent agreement with the pore size distributions calculated from the nitrogen desorption isotherms: 4-20 nm and 4-40 nm for USY and XVUSY, respectively. The large porous area in the USY crystal (Figure 2b, middle left) is not a single pore, but consists of many small cavities separated by thin walls. This explains why no pores larger

than 20 nm are found from the nitrogen adsorption/desorption experiments. The 3D-TEM reconstructions also show that for USY and XVUSY the majority of the mesopores are cavities, although there are also some cylindrical pores connecting the outer surface with the interior of the zeolite crystallite. The shape of the hysteresis loop in the nitrogen physisorption isotherms of USY and XVUSY is indicative for inkbottle type pores combined with cylindrical pores. The cavities visualized with 3D-TEM are most likely connected to the microporous system of the zeolite, thus giving inkbottle type adsorption-desorption behavior in physisorption.

In the cross-section of the 3D-TEM reconstruction of the USY crystal (Figure 2b) also some dark cavities (5–20 nm in diameter) and a dark band (ca. 15 nm thick) on the outer surface are visible. TEM studies have shown that the dark areas inside and outside the crystals of steamed zeolites are most likely amorphous alumina deposited in the mesopores and on the external surface during the steaming process.[7a-c,14] Therefore, we believe that the dark areas in our 3D-TEM reconstruction are not artifacts of the reconstruction, but the imaging of confined material in the mesopores and amorphous alumina deposited on the external surface. In the XVUSY sample no confined material could be detected (Figure 3b), because this has been removed during the severe acid leaching step. When the bulk Si/Al ratio is compared with the surface Si/Al ratio obtained with XPS (Table 1), it is clear that only for USY there is an enrichment of the external surface of the crystals with aluminum. This supports our 3D-TEM observations that only for USY there is a dark band of amorphous alumina on the external surface.

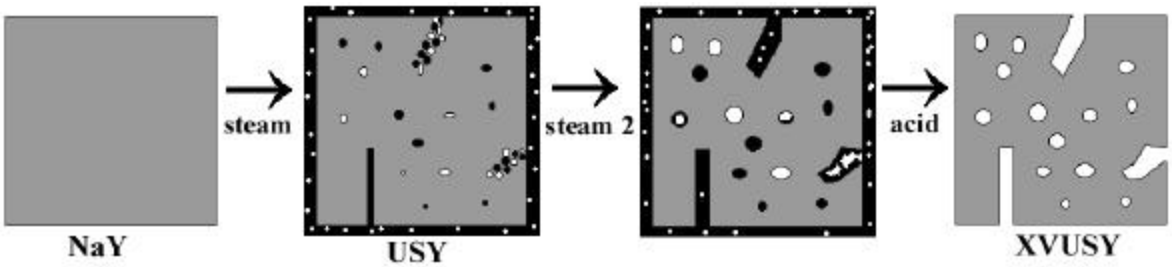

Figure 4: Model for the generation of mesopores in zeolite Y. The zeolite is in gray, the amorphous alumina is black and the empty mesopores are white.

From the 3D-TEM observations we propose a detailed model for the generation of mesopores in dealuminated zeolites (see Figure 4). The model largely supports earlier ones,[15,7a-c] but adds essential new key aspects of mesopore generation. During the steaming process (going from NH_4Y to USY) aluminum ions are extracted from the zeolite lattice and deposited in the micro- and mesopores and on the external surface of the crystals.[16] This is confirmed by the decrease of the zeolite unit cell, the dark areas in the cross-sections of the 3D-TEM reconstruction of USY and the surface enrichment with aluminum of the USY sample as observed with XPS (Table 1). The measured micropore volume for USY is lower than the value expected if all micropores were empty (Table 1: V_{micro} vs. $V^{calc}{}_{micro}$), which indicates that confined material is also present in the micropores. During the extraction of aluminum from the lattice mobile silicon species from defect sites (where aluminum has been extracted) cause some defect sites to develop into cavities in the

zeolite crystals and other defect sites to vanish by healing of the framework. The volume and shape of the mesopores determined by nitrogen physisorption and 3D-TEM confirm this formation of cavities. Thus, the mesoporous system is primarily formed via cavities inside the crystals and not via pores connecting the interior of the crystals with the external surface. During the second steaming step in the generation of XVUSY small cavities close to one another (as visible in Figure 2b) form larger cavities and cylindrical pores, which can be seen from the nitrogen physisorption measurements and 3D-TEM reconstructions. By acid leaching of the steamed sample extraframework aluminum species in the micro- and mesopores and on the external surface area are dissolved.[6,14] This is confirmed by the 3D-TEM reconstruction of XVUSY, which shows neither any confined material in the mesopores nor amorphous alumina on the external surface. Furthermore, XPS shows no surface enrichment in aluminum for XVUSY and the measured and 'expected' micropore volume (Table 1) are on a par. Despite the development of a mesopore system, 2D- and 3D-TEM images show that the crystals remain intact during the steaming and acid leaching steps. Furthermore, the pore size distribution from the nitrogen desorption isotherm of all three samples shows an additional peak at a pore diameter of 70 nm. The fact that this peak, which is caused by the interstitial space between the crystals, is at the same position for all three samples, indicates that the crystals of these samples are of the same order of magnitude. This is different from the results obtained by Beyerlein et al.[7a-c] who claimed extensive fracturing of zeolite Y crystals.

Thus, the pores in a series of dealuminated zeolite Y have been imaged in order to gain insight in the shape and three-dimensional ordering of the mesopores in the zeolite crystallites. Based on the surprising result that most of the mesopores are present as cavities rather than cylindrical pores connecting the external surface with the interior of the crystallite, a more detailed model for the generation of these mesopores is proposed. However, the shape of the mesopores also raises the question to what extent the accessibility and diffusion are enhanced by the formation of these cavities.

Experimental Section

Samples CBV100 (NaY), CBV400 (USY) and CBV780 (XVUSY) were obtained from Shell International Chemicals and Zeolyst. Nitrogen adsorption and desorption measurements were performed at liquid nitrogen temperature on a Micromeritics ASAP 2010. XPS measurements were performed on a Vacuum Generators XPS system using non-monochromatic Al(K_α) radiation at an anode current of 20 mA at 10 keV. For electron microscopy a droplet of a colloidal gold suspension (Sigma, 5 nm gold) was dried on a carbon coated copper grid, thus providing markers for the alignment of the data set. Next, a droplet of a suspension of the sample in ethanol was dried on this grid. From a representative crystal a tilt series of ca. 141 images was taken from about +70° to –70° with 1° intervals at a magnification of 15k or 20k on a Philips CM 200 FEG microscope (200 kV) or on a Tecnai 20 microscope (200 kV), using software for automated electron tomography.[12] From the tilt series a 3D-reconstruction of the crystal is calculated as a stack of thin (1-2 nm) slices.[9-12]

[1] J. M. Thomas, *Angew. Chem.* **1999**, *111*, 3800-3843; *Angew. Chem. Int. Ed.* **1999**, *38*, 3588-3628.
[2] C. C. Freyhardt, M. Tsapatsis, R. F. Lobo, K. Balkus Jr, M. E. Davis, *Nature* **1996**, *295*, 295-298.
[3] A. Corma, V. Fornes, S. B. Pergher, Th. L. M. Maesen, J. G. Buglass, *Nature* **1998**, *396*, 353-356.
[4] S. Mintova, N. H. Olson, V. Valtchev, T. Bein, *Science* **1999**, *283*, 958-960.
[5] C. J. H. Jacobsen, C. Madsen, J. Houzvicka, I. Schmidt, A. Carlsson, *J. Am. Chem. Soc.* **2000**, *122*, 7116-7117.
[6] J. Scherzer, *ACS Symp. Ser.* **1984**, *248*, 157.
[7] a) C. Choi-Feng, J. B. Hall, B. J. Huggins, R. A. Beyerlein, *J. Catal.* **1993**, *140*, 395-405. b) C. Choi-Feng, J. B. Hall, B. J. Huggins, R. A. Beyerlein, *ACS Symp. Ser.* **1994**, *571* (Fluid Catalytic Cracking III), 81-97. c) R. A. Beyerlein, C. Choi-Feng, J. B. Hall, B. J. Huggins, G. J. Ray, *Top. Catal.* **1997**, *4*, 27-42. d) Y. Sasaki, T. Suzuki, Y. Takamura, A. Saji, H. Saka, *J. Catal.* **1998**, *178*, 94-100.
[8] A. Carlsson, M. Kaneda, Y. Sakamoto, O. Terasaki, R. Ryoo, S. H. Joo, *J. Electron Microsc.* **1999**, *48*, 795-798.
[9] A. J. Koster, U. Ziese, A. J. Verkleij, A. H. Janssen, K. P. de Jong, *J. Phys. Chem. B.* **2000**, 104, 9368-9370.
[10] J. Frank, *Electron Tomography*, Plenum Press, New York, **1992**.
[11] A. J. Koster, U. Ziese, A. J. Verkleij, A. H. Janssen, J. de Graaf, J. W. Geus, K. P. de Jong, *Stud. Surf. Sci. Catal.* **2000**, *130*, 329-334.
[12] A. J. Koster, R. Grimm, D. Typke, R. Hegerl, A. Stoschek, J. Walz, W. Baumeister, *J. Struct. Biol.* **1997**, *120*, 276-308.
[13] P. Hudec, J. Novansky, S. Silhar, T. N. Trung, M. Zubek, J. Madar, *Ads. Sci. Tech.* **1986**, *3*, 159-166.
[14] J. Lynch, F. Raatz, P. Dufresne, *Zeolites* **1987**, *7*, 333-340.
[15] C. Marcilly, *Pet. Tech.* **1986**, 328, 12-18.
[16] M. J. Remy, D. Stanica, G. Poncelet, E. J. P. Feijen, P. J. Grobet, J. A. Martens, P.A. Jacobs, *J. Phys. Chem. B*, **1996**, *100*, 12240-12447.